GHRS Photocathode Blemishes: Discoveries Lurking in the Spectrum

Glenn M. Wahlgren[1], Jennifer L. Sandoval[1] and Don J. Lindler[2]

Abstract

Blemishes and irregularities in the photocathode and window materials of the GHRS digicon detectors produce spurious features that are a source of noise in the spectrum. An iterative computational technique is applied to GHRS data obtained with the FP-SPLIT option to create a granularity vector that represents the fixed pattern noise of the observation. At signal-to-noise levels less than 100 the granularity vector is used to detect and remove blemishes in a data set of first-order grating spectra of the bright star Sirius-A.

I. Nature of the Problem

Congratulations! You were awarded *HST* observing time to obtain spectra with the Goddard High Resolution Spectrograph (GHRS). The data was acquired in a routine fashion and your data tapes have arrived. You can match the STScI supplied reduced data files with your theoretical spectrum, or, if you are ambitious you first re-reduce the data with software obtained from STScI or the GHRS IDT. Either way, the data is reduced in a rather straightforward, cookbook manner. Comparison of modelled data with the observation reveals a rather deep unidentified feature in the observation. You feel you may have discovered 'cathodium,' because although you have followed each reduction procedure as prescribed you have not inspected the intermediate-step data products.

The ultraviolet spectrum of most astronomical sources is difficult enough to understand without having to worry about features that in reality do not exist. However, that is precisely what one needs to do with any GHRS spectrum before one can feel confident about its interpretation. There are several ways in which undesirable discrete features and distortions can arise in the data: individual diode response (both high and low), sleaks, blemishes, or poor doppler compensation correction. In this paper we illustrate the effect of photocathode blemishes on the spectrum; their detection and removal.

II. GHRS Photocathodes and Blemishes

The GHRS is comprised of two separate detector and electronics chains, or sides, that are essentially different only by the coatings of their photocathode (pc) windows. Each pc active area is 18 x 26 mm in size, and accommodates the 25 mm length of the

1. Computer Sciences Corporation, Code 681, GSFC, Greenbelt, MD 20771
2. Advanced Computer Concepts, Code 681, GSFC, Greenbelt, MD 20771

diode array at the opposite end of the detector assembly. The side 1 pc window is a 4 mm thick piece of lithium fluoride (LiF) with a cesium iodide (CsI) photocathode. The side 2 pc window is a 3 mm thick magnesium fluoride (MgF_2) window with a cesium telluride (CsTe) photocathode. Side 1 sensitivity allows it to be most efficient between 1050 – 1700 Å and is associated with the use of the G140L and G140M gratings and echelle-A, while side 2 is sensitive over the entire 1100 – 3300 Å range and utilizes the G160M, G200M, and G270M gratings and echelle-B for science operations. Photons directed from one of the gratings on the carrousel impinge upon the associated pc window and liberate electrons that are then directed to the diode array by the magnetic fields of the detector. The pc location sampled by a diode is a function of the specified grating and wavelength, as well as a variable thermal and geomagnetic spacecraft environment. Therefore, two similar observations with the same specified grating and wavelength may not sample the same location on the pc. GHRS instrument descriptions at various levels of complexity can be found in TePoel (1985), Cushman, Ebbets, & Holmes (1986), Ebbets (1992), and Soderblom (1993).

Photocathode blemishes are, in part, a natural result of the physical and chemical properties of the materials employed and the technology that is used to construct optical components. The blemishes are localized physical deformities in the pc material, often referred to as scratches or digs, that are registered as a deficiency of counts by elements of the silicon diode array. They are a subset of the more generically termed fixed-pattern noise (fpn) pc window related response deficiencies which affect the spectrum over a larger area of the pc window. The fpn essentially limits the effective spectral signal-to-noise level at high counts. Cardelli (this volume) discusses fpn and its removal from GHRS spectra for the case where high count totals are obtained. However, at S/N levels that are limited by photon statistics the low-level fpn will not be evident. The impression should not be formed that high count totals are required for the identification and removal of spurious spectral features. The strong discrete blemishes will still be evident at S/N levels under 100 and can be removed.

Several processes can affect the creation and evolution of blemishes and fpn. Among them:

- Humidity has been found to decrease the transmittance of LiF windows, particularly below 1600 Å (Patterson & Vaughn 1963). The transmittance loss is due to a surface film formed on the crystal by chemical reaction products of H_2O with LiF. Tests show that after an initial throughput loss has developed, exposure to vacuum conditions accelerates the loss. Woodruff (1978a) has cautioned that in-orbit (vacuum) exposure of the windows should be kept in mind during the GHRS calibration phase. The limited use of the GHRS side-1 prior to the *HST* servicing mission makes it imperative that its potential use in the post GHRS-Redundancy Unit environment allow for proper re-calibration and continued sensitivity monitoring. MgF_2 windows, such as that on side-2, have not been found to be affected by humidity.

- Crystal flaws can contribute to variations in transmittance over the surface of the window. Cleaved surfaces also result in a certain amount of scattered light. The GHRS windows are a dual plane window design with polished surfaces. Sleaks can result from the polishing process.

- Surface scratches and digs, on both the window and pc sides, can result from handling during the manufacture and assembly phases. Pre-flight tests (Eck 1983) with detector 2 observed a few digs, of size 400-600 μm x 600 μm, after reassembly of the unit following design changes. Scratches that cover a full diode width can either degrade or make unusable the particular diode response that samples that portion of the pc (Woodruff 1978b). Large digs, such as mentioned above, can affect the response of up to eight diodes. The presence of particulate contamination will likewise obscure specific diodes.

Pre-flight testing of spare digicons from the GHRS tube flight build were conducted to test pc quantum efficiency variations (Beaver & Greenwell 1989). The long shelf-time of the detectors, forced by *HST* launch delays, had raised concerns of sensitivity loss. Two spare digicons, with pc characteristics of the two flight units, were tested and found not to show sensitivity loss that would be indicative of a generic problem with the flight build. An additional CsTe pc digicon, referred to as Engineering Model 1 (EM1) and not of the exact flight build design, did show a significant drop in sensitivity over the time period 1980 - 1987. While it is only speculated as to why the EM1 unit suffered a sensitivity loss, it does point out that digicon tubes can develop individual problems.

III. Blemish Removal

Removal of pc blemishes can be incorporated as an additional step in the normal data reduction procedure. The assumption, however, is that the data have been obtained with the GHRS FP-SPLIT[1] option. The FP-SPLIT option forces the observation to be broken into either 2 or 4 subexposures, where the GHRS grating carrousel has been moved a slight amount between subexposures in order that each diode of the array samples a slightly different position of the pc. The effects from low-level fpn can be reduced nominally by a factor of two by shifting and coadding when four individual FP-SPLIT subexposures are available. The larger blemishes can appear as either 2 or 4 spectral absorption features that are slightly displaced from each other, by the wavelength equivalent of one carrousel step, when all subexposures are overplotted in wavelength space. For all work regarding removal of fpn and blemishes we recommend that the observations be obtained using FP-SPLIT= 4.

We have employed a technique (Lindler 1991) that iteratively computes the fpn pattern and corrects for fpn in the source flux as the solution of an over-determined non-linear system of equations. The input data are multiple spectra aligned by shifting in the dispersion direction, with the assumption of the same fpn pattern. The procedure involves:

- initially setting the fpn (granularity) vector elements to unity
- correct (divide) each raw observation by the granularity vector
- compute a new flux array by shifting and averaging the corrected raw observations

1. see Proposal Instructions.

- compute a new granularity vector for each raw observation using the new flux array
- compute a new granularity vector by averaging the individual granularity vectors.

This process, from the second step, is iterated until a convergence criterion is met. Final solutions may display 'ringing' if a nearly constant value for the spectrum offsets is used, or spectral features are not perfectly registered. However, the GHRS grating carrousel tends to produce unequally offset spectra from the FP-SPLIT option. In reality, limitations to the technique are imposed by spatially variable fpn, near equally spaced offsets, and the occurrence of near equally spaced source absorption features. Any will increase the noise level in the iterated flux and granularity vectors. The technique is particularly successful at high S/N levels in removing fpn from the flux spectrum (Cardelli, this volume). At lower S/N, where counting statistics dominate the errors, this technique produces signal level dependent errors that are larger than those from the simple shift and coadd technique, and should therefore be used only to make use of the granularity vector to locate blemishes to be masked from the spectrum.

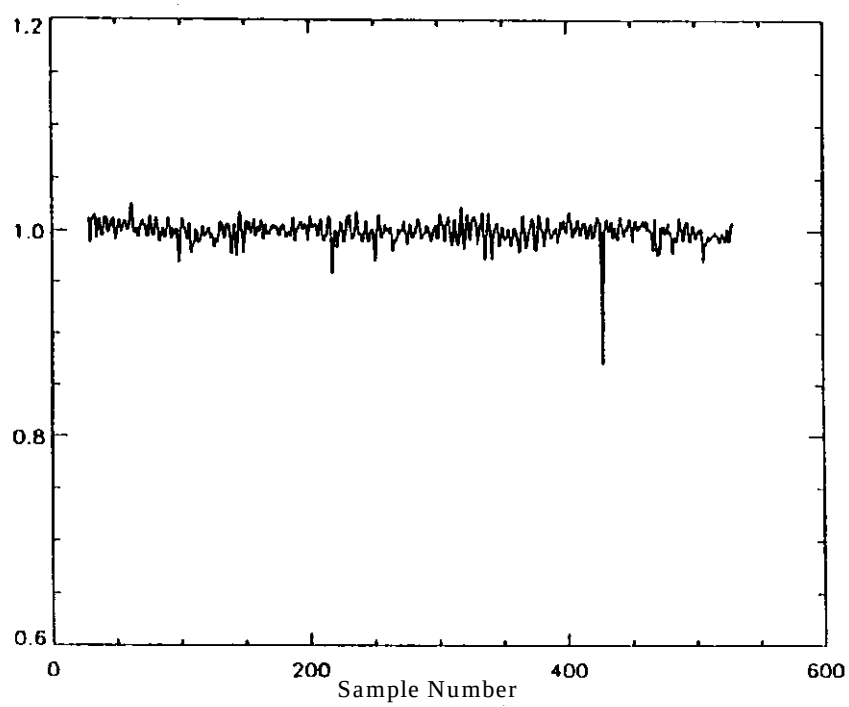

Figure 1: Granularity vector. Note obvious blemish near sample position 430.

Visual inspection of the iteration program granularity vector (Figure 1) allows the user to select the level of blemish that is required for data interpretation. For each pc a coordinate grid is constructed having grid spacings of 50 μm in both the X (*sample*) and Y (*line*) dimensions. The origin of the grid is the upper-left corner of the pc. Simple linear relations have been calibrated that relate the commanded deflections in both X and Y coordinates to *sample, line* values. The *sample, line* values for an

observation can be computed using information extracted from the observation Science Header Packet. In Figure 1 it is evident that a blemish exists near *sample* position 430. Interactive techniques, such as our use of IDL, can be used to measure the *sample* range from such a plot. We have assumed that the blemish extends by ±1 unit in *line* position. For each blemish the *line* and *sample* ranges are determined and a blemish table can be constructed for individual observation data sets. It is important that each blemish be assigned an epsilon (data quality flag) value that is appropriate for its severity. In GHRS IDT data reduction software, a value of 150 for the *badeps* parameter corresponds to a blemish that is at most 5 percent deep, and a value of 180 for depths greater than 5 percent.

To remove the effects from blemishes the GHRS spectrum is first reduced to produce the individual wavelength and flux calibrated FP-SPLIT spectra. Running the IDL routine HRSMERGE (available from the GHRS IDT), with optional parameter *badeps* set to the value of the epsilon level that needs to be removed, will align and coadd the FP-SPLIT segments, excluding the *sample/line* ranges designated in the specified blemish table. One drawback is that the S/N level for the affected data points will be reduced, by a factor of 1.154 in the case where three of four FP-SPLIT spectra are useful.

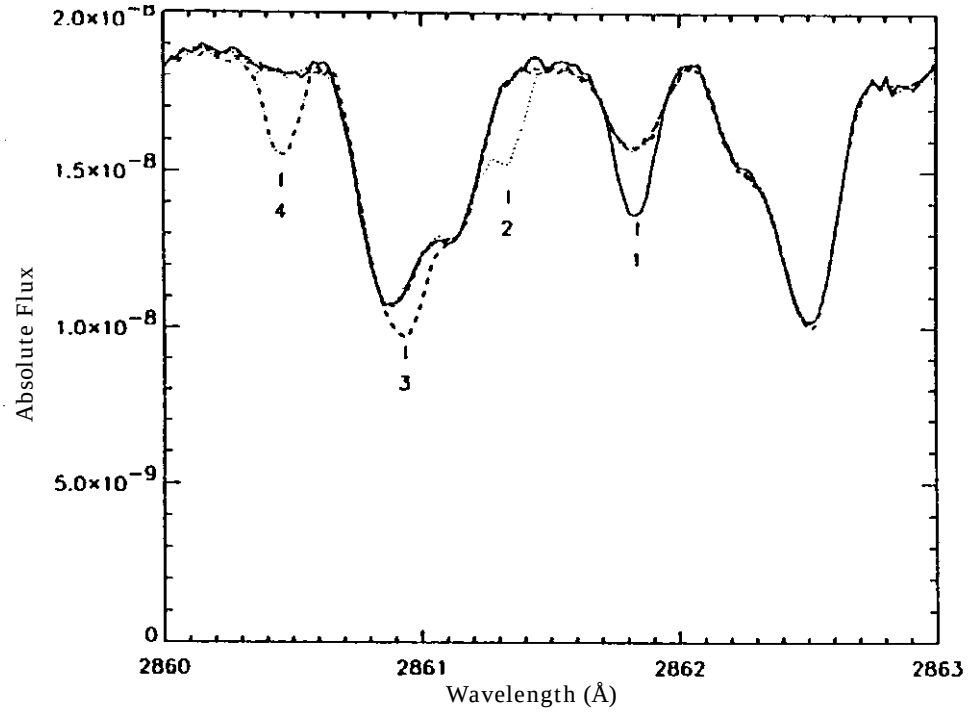

Figure 2: Overplots of individual FP–SPLIT spectra of Sirius with locations numbered of spectral features resulting from the blemish at *sample* 430.

The effect upon the spectrum of the blemish near *sample* position 430 is shown in Figure 2. The 3 Å of data presented represents approximately 7 percent of the observation wavelength range. Each of the four individual FP-SPLIT segments is plotted using different linestyles and the corresponding four spectral features resulting from the single blemish are numbered. For this blemish the additional

features are obvious in the FP-SPLIT segments but not necessarily in the final merged spectrum. Figure 3 presents the final merged (coadded) spectra both with (solid line) and without (dashed line) removal of the blemish. For FP-SPLIT segments 1, 2, and 3 an analysis of the uncorrected spectrum might produce increased abundances for the contributing elements or lead to concerns regarding their oscillator strengths. FP-SPLIT segment 4 might lead to the identification of an elemental species that does not exist in the star. Other blemishes will produce spectral features that are more or less obvious in the individual FP-SPLIT segments than those presented here and it should be remembered that searching the final merged spectrum will not necessarily uncover these features. *Observations taken without the FP-SPLIT option provide no information for identifying and removing blemishes.*

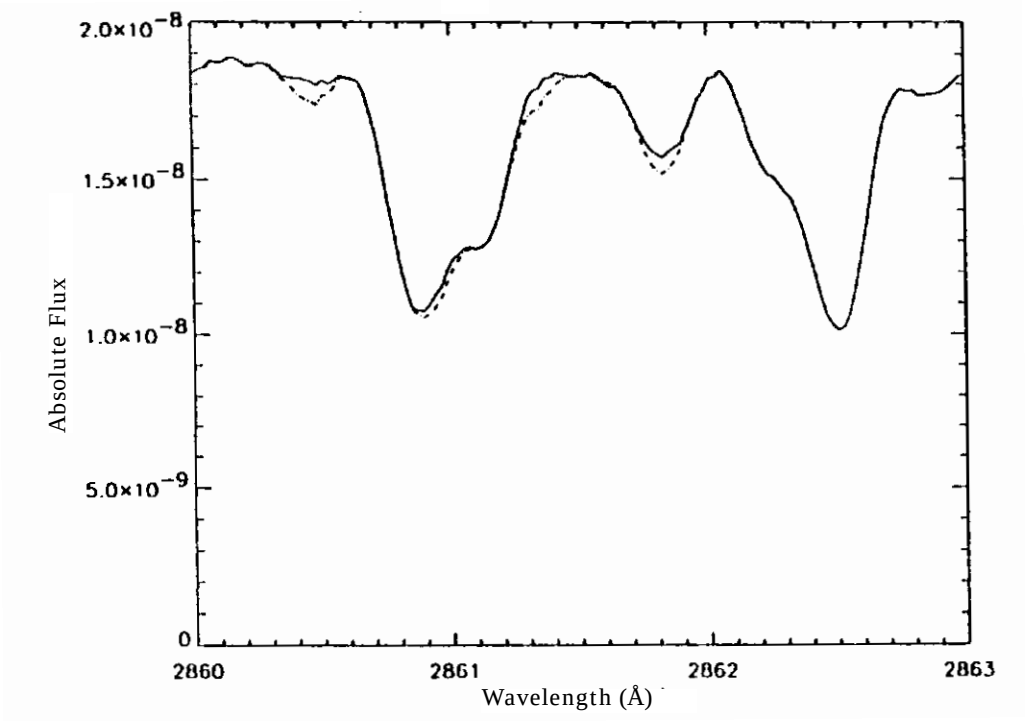

Figure 3: Coadded spectra for cases where blemish has (solid) and has not (dashed) been removed.

IV. Discussion

In the OV/SV planning phases for GHRS calibration, tests were constructed that would collect data to allow for a partial mapping of the two GHRS photocathodes. This proposal was never executed and after early observations were vigorously analyzed (Cardelli 1991) it was recommended that the use of FP-SPLIT will allow for the removal of detector effects (Ebbets 1992). A first post-launch mapping of the photocathodes was constructed by Robinson (1991) using Science Verification flux calibration spectra of the bright early-type star μ Columbae (O9.5 V), obtained with the first-order gratings. Blemishes were detected by comparing the overlap regions of contiguous spectra. The μ Col calibration data were not obtained using FP-SPLIT and so can not be analyzed by the iterative scheme outlined in section 3. The detection of blemishes in the μ Col data set is not considered complete.

The recently acquired first-order grating spectral atlas of Sirius-A (Wahlgren et al. 1993) provides a large data set that can be used to supplement the earlier work of Robinson. The Sirius spectra were obtained with the FP-SPLIT = 4 option and have been searched for blemishes with the iterative technique discussed above.

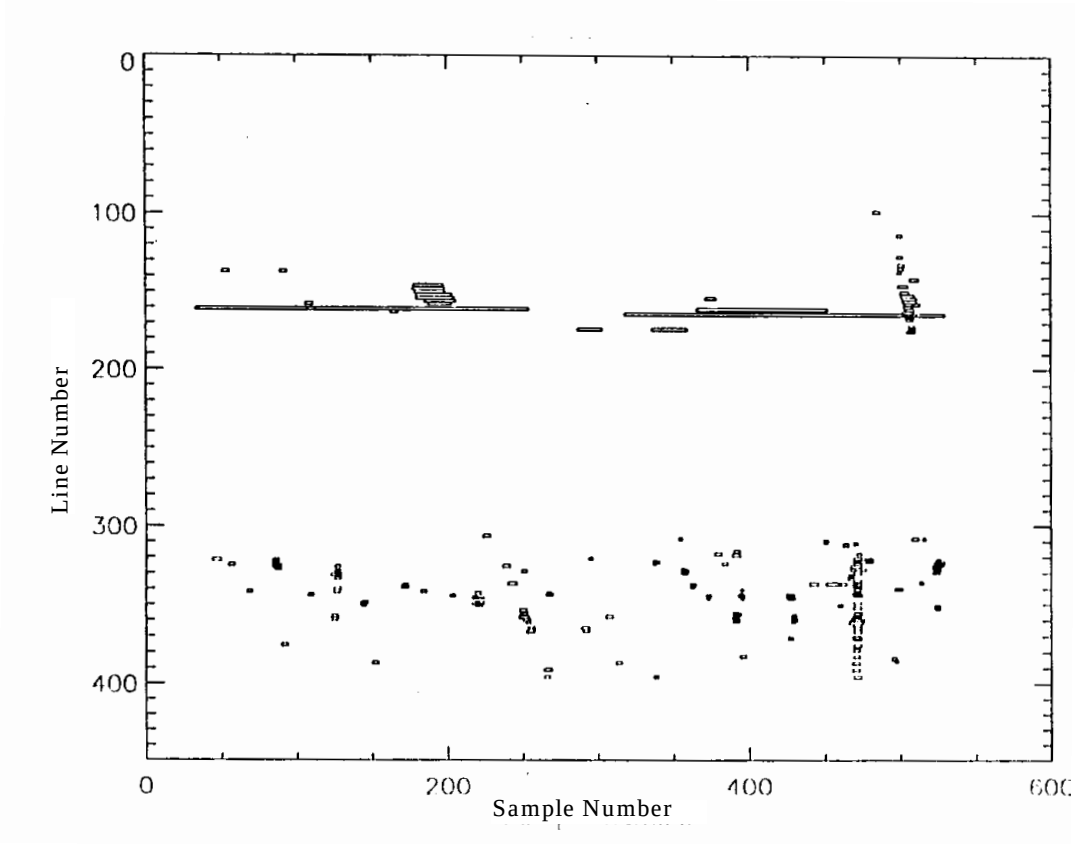

Figure 4: Areal coverage of GHRS photocathodes by catalogued blemishes.

Figure 4 presents all of the catalogued blemishes, from both data sets. The entire range of a pc is represented by the *line* and *sample* ranges plotted. The figure is actually a composite from both detectors. Data plotted in the *line* range of 100 - 200 are from the G140L and G140M gratings of side 1 while the data in the *line* range of 300 - 400 are from the side 2 gratings G160M, G200M, and G270M. Echelle formats for each detector cover the entire pc format but the first-order gratings are restricted. The limited amount of side 1 data originates only from the μ Col calibration observations. The long horizontal features identified with detector 1 are difficult to refer to as blemishes, but do not appear to result from simple vignetting. Both detectors show a vertical feature, likely to be scratches, at high sample numbers. Smaller extended features are also noticeable.

Figure 5 expands the detector 2 data and distinguishes between μ Col (boxes) and Sirius (stars). The symbol sizes are approximately the same as the area boxes in Figure 4 and are plotted for the center of the *line*, *sample* ranges. Many features were

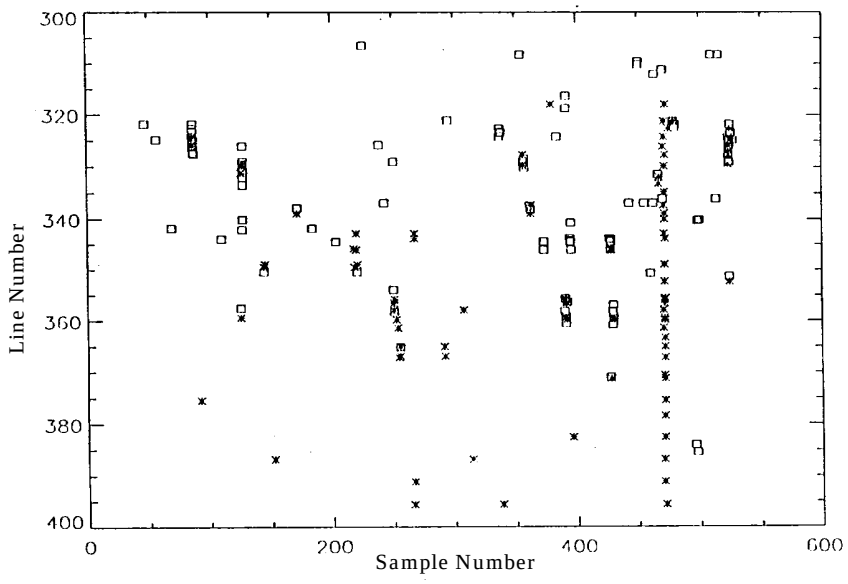

Figure 5: Detector 2 blemishes obtained from μ Col (squares) and Sirius (stars) data sets.

observed by both data sets, and tend to produce most of the deepest features in the iterative-scheme output. It is also clear that the two data sets do not have fulloverlap. However, there are features that were observed in only one of the data sets and can not be explained by various selection effects. It is possible that pc blemishes evolve with time. For this possible reason alone the construction of photocathode maps for the removal of fpn features is not feasible.

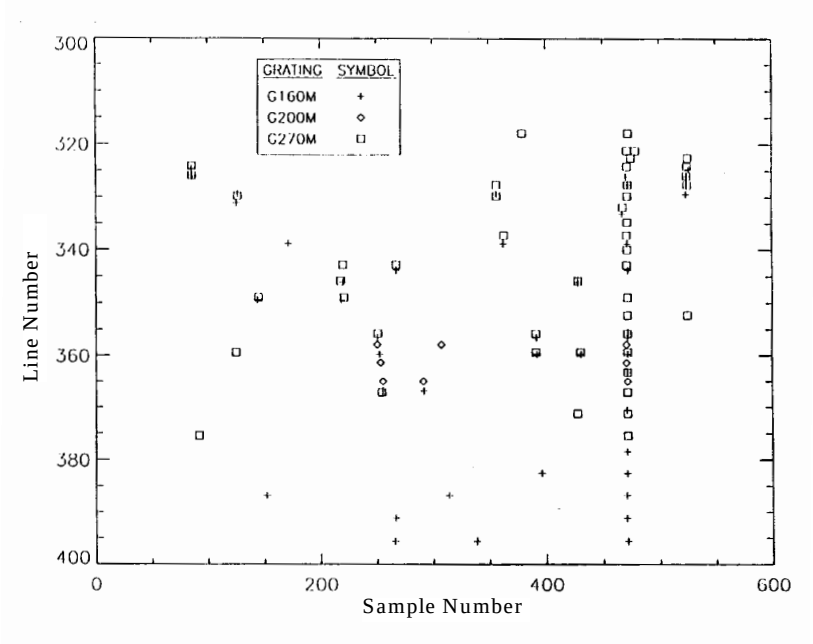

Figure 6: Sirius data set blemishes broken down by grating.

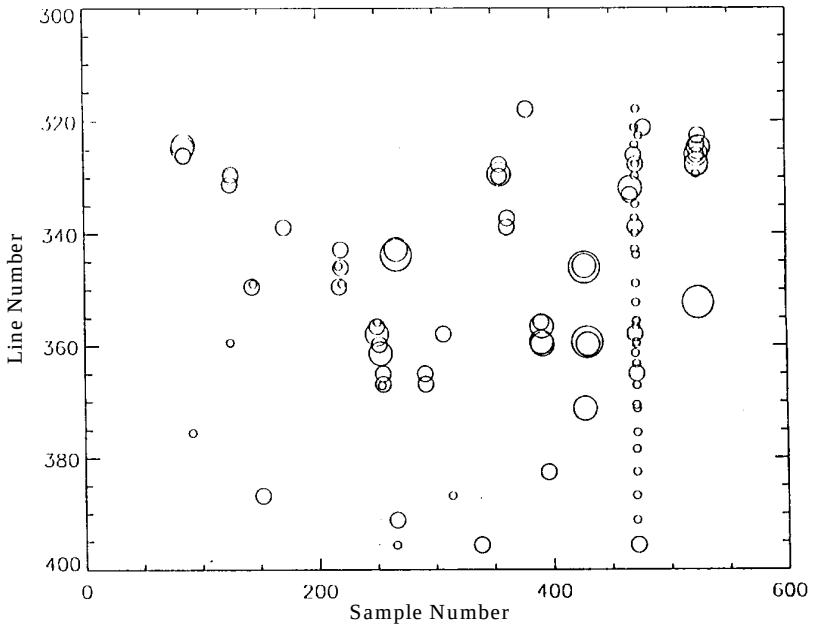

Figure 7: Sirius data set blemishes. Circle size depicts blemish depth (1-4, 5-10, 10-20, and 20-40 percent) in granularity vector, not necessarily photocathode blemish size.

Figures 6 and 7 present information regarding the Sirius data set alone. The extent of the separate gratings is presented in Figure 6, showing the overlap on the pc for the three gratings and the fact that, for the most part, where *line* positions for different observations/gratings are available they tend to identify the same blemish. For these same blemishes Figure 7 illustrates their approximate strengths, or feature depths in percent from the continuum level, in the iterative scheme output. The long vertical scratch-like feature located near *sample* number 470 is not strong and may explain why it was not identified in the μ Col data set.

References

Beaver, E., & Greenwell, D., 1989, BALL System Engineering Report (SER) GHRS-DET-130, 'Recent GHRS Quantum Efficiency Data'

Cardelli, J., 1991, BALL SER GHRS-SV-113, 'Detailed Analysis of Photocathode FPN Granularity, S/N Limits, and Weak Line Detectability Using the GHRS Detector Systems'

Cushman, G., Ebbets, D., & Holmes, A., 1986, 'Pre-Launch Calibration Report for the High Resolution Spectrograph for the Hubble Space Telescope,' HRS-2176-051, BALL Aerospace Systems Group

Ebbets, D., 1992, 'Final Report of the Science Verification Program for the Goddard High Resolution Spectrograph for the Hubble Space Telescope,' BALL Aerospace Systems Group

Eck, H., 1983, BALL SER DET-103, 'D2-MkIII Performance Summary'

Lindler, D.J., 1991, BALL SER GHRS-SV-102, 'Removal of FPN from FP-SPLIT Observations'

Patterson, D.A., & Vaughn, W.H., 1963, JOSA, 53, 851

Robinson, R.D., 1991, BALL SER GHRS SV-080, 'Small Scale Imperfections in the GHRS Detectors and Their Influence on Observations'

TePoel, H.E., 1985, 'SI System Description and User's Handbook for the High Resolution Spectrograph for the Hubble Space Telescope,' HRS-2176-050C (SE-01), BALL Aerospace Systems Group

Soderblom, D.R., 1993, 'Instrument Handbook for the GHRS,' (STScI:Baltimore)

Wahlgren, G.M., Johansson, Se., Kurucz, R.L., & Leckrone, D.S., 1993, BAAS, in press, 'A GHRS/*HST* Spectral Atlas of Sirius-A'

Woodruff, R., 1978a, BALL SER OPT-023, 'Data on Environmental Effects on LiF Crystals' Woodruff, R., 1978b, BALL SER OPT-013, 'Digicon Window Optical Constraints: Thickness, Polish, Scratch-Digs'